Wuhan University Journal of Natural Sciences

2023, Vol.28 No.5, 411-420

Article ID 1007-1202(2023)05-0411-10

DOI https://doi.org/10.1051/wujns/2023285411

Uniform Convergence Analysis of the Discontinuous Galerkin Method on Layer-Adapted Meshes for Singularly Perturbed Problem

□ **SHI Jiamin, LU Zhongshu, ZHANG Luyi, LU Sunjia, CHENG Yao**†

School of Mathematical Sciences, Suzhou University of Science and Technology, Suzhou 215009, Jiangsu, China

Abstract: This paper concerns a discontinuous Galerkin (DG) method for a one-dimensional singularly perturbed problem which possesses essential characteristic of second order convection-diffusion problem after some simple transformations. We derive an optimal convergence of the DG method for eight layer-adapted meshes in a general framework. The convergence rate is valid independent of the small parameter. Furthermore, we establish a sharper L^2-error estimate if the true solution has a special regular component. Numerical experiments are also given.

Key words: layer-adapted meshes; singularly perturbed problem; uniform convergence; discontinuous Galerkin method

CLC number: O241

0 Introduction

Singularly perturbed problems attract much attention in such applications as optimal control, chemical reactions, fluid dynamics and electrical networks[1]. The exact solution generally displays boundary layers which causes many numerical difficulties to the traditional finite element method on the quasi-uniform mesh. To obtain satisfactory numerical approximations, several numerical strategies were developed, such as the layer-adapted meshes, the fitted operator methods and the stabilised numerical method, see Refs. [1-3] for a survey.

Discontinuous Galerkin (DG) method is a finite element method whose test function and trail function have possible discontinuous points at the element edges[4]. As such, the discontinuous finite element space provides much flexibility in solving those problems exhibiting large gradients, boundary layers or even discontinuous interfaces, see Ref. [5] for a survey.

For the singularly perturbed problem whose solution exhibits boundary layers, numerical investigations were performed in Ref. [6] for the DG method. Local behavior was explored on the uniform mesh. Uniform convergence and superconvergence were observed on Shish-

Received date: 2023-03-02

Foundation item: Supported by the National Natural Science Foundation of China (11801396) and National College Students Innovation and Entrepreneurship Training Project (202210332019Z)

Biography: SHI Jiamin, female, Undergraduate, research direction: computational method. E-mail: 21200210103@qq.com

†To whom correspondence should be addressed. E-mail: ycheng@usts.edu.cn

kin mesh. Along this direction, research on the DG method for singularly perturbed problems was developed in a series of papers, see Refs. [7-10].

However, the above error estimates are often performed on Shishkin mesh, which has a simple structure. Owing to the influence of a logarithmic factor, the convergence rate will be deteriorated as the degree of piecewise polynomials goes larger. It is therefore of much interest to derive optimal convergence rate on general graded layer-adapted meshes. Recently, we studied the local DG method on several layer-adapted meshes. Some uniformly optimal error estimates were established for second order convection-diffusion problem[11,12].

This paper concerns a uniform convergence of the DG method under a much larger range of the layer-adapted meshes. These meshes contain five common Shishkin-type meshes as well as three common Bakhvalov-type meshes[13,14]. Based on a general analysis framework, we establish optimal convergence for the DG method independent of small perturbation parameter. In particular, we establish a sharper L^2-norm convergence rate under the situation that the smooth component of the true solution is a piecewise polynomial. Some numerical results are given to confirm our prediction.

We organize this paper as follows. First, layer-adapted meshes and the DG method are introduced in Section 1. Then we present a local projector as well as its approximation error. Our main result follows in Section 2. Finally, we supplement some numerical results to validate our error estimate.

1 Layer-Adapted Meshes and the DG Method

Consider a one-dimensional model problem

$$\begin{cases} -\varepsilon q' + aq = f \quad \text{in } \Omega = (0,1) \\ q(1) = 1 \end{cases} \tag{1}$$

which possesses some essential characteristics of the following second-order problem

$$\begin{cases} -\varepsilon u'' + au' + bu = f \ \text{ in } \Omega = (0,1) \\ u'(1) = 1, \ \ u(0) = 0 \end{cases} \tag{2}$$

In fact, one can transform (2) into a problem with $b=0$ if a and b are both constants. Then introduce the following transformation

$$u' = q, \quad u(0) = 0$$

one obtains the model problem (1).

Assume that $a \geqslant \alpha > 0,$ problem (1) exhibits a boundary layer at $x=1$. Assume that the exact solution of (1) can be expressed as[15]

$$q(x) = q(1)\,\mathrm{e}^{\int_1^x a(s)/\varepsilon \mathrm{d}s} + \int_x^1 \varepsilon^{-1} f(t)\,\mathrm{e}^{\int_t^x a(s)/\varepsilon \mathrm{d}s}\mathrm{d}t$$

which implies a decomposition $q = \bar{q} + q_\varepsilon$. Here $\bar{q}$ is the regular component and q_ε is the layer component satisfying

$$\left|\bar{q}^{(j)}(x)\right| \leqslant C, \ \left|q_\varepsilon^{(j)}(x)\right| \leqslant C\varepsilon^{-j}\mathrm{e}^{-\alpha(1-x)/\varepsilon}, \ \ \forall j = 0, 1, \cdots, k+1 \tag{3}$$

1.1 Layer-Adapted Meshes

Let φ be a monotonically increasing, continuous and piecewisely differentiable function. Let $\varphi(0)=0$. Introduce a mesh transition parameter

$$\tau := \min\left\{\frac{1}{2}, \frac{\sigma\varepsilon}{\alpha}\varphi\left(\frac{1}{2}\right)\right\}$$

where $\sigma > 0$ is a constant. Assume that $\tau = \sigma\varepsilon\varphi(1/2)/\alpha$ for a small ε. Otherwise, the problem is non-singularly perturbed and one can carry out the error analysis in a classical framework. Let $N \geqslant 2$ be an even integer. Denote $\Omega = \Omega^c \cup \Omega^f$, where $\Omega^c = [0, 1-\tau]$ is the rough region and $\Omega^f = [1-\tau, 1]$ is the refined region; they have both equal elements. The mesh points are given by

$$x_j = \begin{cases} \dfrac{2j}{N}(1-\tau), & j = 0, 1, \cdots, \dfrac{N}{2} - 1 \\ 1 - \dfrac{\sigma\varepsilon}{\alpha}\varphi(1 - \dfrac{j}{N}), & j = \dfrac{N}{2}, \dfrac{N}{2} + 1, \cdots, N \end{cases} \tag{4}$$

In Table 1, we list eight common layer-adapted meshes, which are simplified as S-, BS-, mBS-,VS-, pS-, B-, mVB- and RS-meshes. Here $\psi = \mathrm{e}^{-\varphi}$ is mesh characterizing function. See Ref. [13] for more details.

Table 1 Layer-adapted meshes

mesh	$\varphi(t)$	$\psi(t)$	$\max\lvert\psi'(t)\rvert$
S	$2t\ln N$	N^{-2t}	$2\ln N$
BS	$-\ln\left(1-2(1-N^{-1})t\right)$	$1-2(1-N^{-1})t$	2
mBS	$t/(1/2+1/\left(2\ln N\right)-t)$	$\mathrm{e}^{-t/(1/2+1/(2\ln N)-t)}$	$8\mathrm{e}^{-1}$
VS	$2t\ln N/(1+\left(1-2t\right)\ln N)$	$\mathrm{e}^{-2t\ln N/(1+(1-2t)\ln N)}$	$8\mathrm{e}^{-1}$
pS	$\left(2t\right)^m\ln N$	$N^{-(2t)^m}$	$C\left(\ln N\right)^{1/m}$
B	$-\ln\left(1-2(1-\varepsilon)t\right)$	$1-2(1-\varepsilon)t$	2
mVB	$t/\left(1/2+1/(2\ln\varepsilon^{-1})-t\right)$	$\mathrm{e}^{-t/(1/2+1/(2\ln\varepsilon^{-1})-t)}$	$8\mathrm{e}^{-1}$
RS	$\ln\left(1+(N-1)(2t)^l\right)$	$\left(1+(N-1)(2t)^l\right)^{-1}$	$CN^{1/l}$

Set $\Omega_N=\{I_j\}_{j=1}^N$, where each element $I_j=(x_{j-1},x_j)$ has the mesh size $h_j=x_j-x_{j-1}$. Assume that $\varepsilon\leqslant N^{-1}$, then one has $\psi(1/2)\leqslant N^{-1}$ for each mesh in Table 1. This property will be frequently used in the following analysis.

Lemma 1[12] Define

$$\mathcal{G}_j=\min\left\{\frac{h_j}{\varepsilon},1\right\}\mathrm{e}^{-\alpha(1-x_j)/\sigma\varepsilon},\quad j=N/2+1,\cdots,N$$

Then one has

$$\max_{N/2+1\leqslant j\leqslant N}\mathcal{G}_j\leqslant CN^{-1}\max|\psi'|$$

$$\sum_{j=N/2+1}^{N}\mathcal{G}_j\leqslant C$$

Here $C>0$ does not depend on ε and N.

1.2 The DG Method

Define a finite element space as

$$V_N=\left\{z\in L^2(\Omega): z|_{I_j}\in P^k(I_j),\ \ \forall I_j\in\Omega_N\right\}$$

where $P^k(I_j)$ is a space of polynomial with degree no larger than k. The functions in the above discontinuous finite element space have possible discontinuous points at the cell ends. Define $z_j^{\pm}=\lim\limits_{x\to x_j^{\pm}}z(x)$ and the jumps as

$$[\![z]\!]_0=z_0^+,\quad [\![z]\!]_j=z_j^+-z_j^-,\ j=1,\cdots,N-1,$$
$$[\![z]\!]_N=-z_N^-.$$

The DG method reads: Find $Q\in V_N$ such that

$$\int_{I_j}Q(\varepsilon r'+ar)\mathrm{d}x-\varepsilon\hat{Q}_jr_j^-+\varepsilon\hat{Q}_{j-1}r_{j-1}^+=\int_{I_j}fr\mathrm{d}x \qquad (5)$$

holds for any $r\in V_N$ and $I_j\,(j=1,2,\cdots,N)$, where

$$\hat{Q}_j=\begin{cases}Q_j^+, & j=0,1,\cdots,N-1\\ q(1), & j=N\end{cases}$$

Denote $\left\langle\varphi,\phi\right\rangle:=\sum\limits_{j=1}^{N}\left\langle\varphi,\phi\right\rangle_{I_j}:=\sum\limits_{j=1}^{N}\int_{I_j}\varphi\phi\mathrm{d}x$. Rewrite the scheme (5) into a compact form: Find $Q\in V_N$ such that

$$B(Q;r)=\left\langle f,r\right\rangle+\varepsilon q(1)r_N^-,\quad \forall r\in V_N \qquad (6)$$

where

$$B(Q;r)=\left\langle Q,\varepsilon r'+ar\right\rangle+\varepsilon\sum_{j=1}^{N-1}Q_j^+[\![r]\!]_j+\varepsilon Q_0^+r_0^+.$$

One obtains an energy norm

$$\|Q\|_{\mathrm{E}}^2:=B(Q;Q)=\|a^{1/2}Q\|^2+\frac{\varepsilon}{2}\sum_{j=0}^{N}[\![Q]\!]_j^2$$

Let $f=q(1)=0$ in (6) then one has $B(Q;Q)=\|Q\|_{\mathrm{E}}^2=0$ and $Q=0$, which implies the uniquely existence of the computed solution determined by the DG method (6).

2 Convergence Analysis

Divide the error $e=q-Q$ as follows

$$e=\left(q-\pi^+q\right)-\left(Q-\pi^+q\right):=\eta-\xi$$

where $\pi^+: H^1(\Omega_N)\to V_N$ is the local Gauss-Radau projecter such that for any function $z\in H^1(\Omega_N)$ and each element I_j,

$$(\pi^+z)_{j-1}^+=z_{j-1}^+,\quad \left\langle\pi^+z,v\right\rangle_{I_j}=\left\langle z,v\right\rangle_{I_j},\quad \forall v\in P^{k-1}(I_j) \qquad (7)$$

From Ref. [16], one can verify the well-posedness of the above projection. Furthermore,

$$\|\pi^+z\|_{I_j}\leqslant C\left[\|z\|_{I_j}+h_j^{1/2}|z_{j-1}^+|\right] \qquad (8)$$

$$\|\pi^+z\|_{L^\infty(I_j)}\leqslant C\|z\|_{L^\infty(I_j)} \qquad (9)$$

$$\|z-\pi^+z\|_{L^\ell(I_j)}\leqslant Ch_j^{k+1}\|z^{(k+1)}\|_{L^\ell(I_j)},\quad \ell=2,\infty \qquad (10)$$

Lemma 2 Assume $\sigma\geqslant k+1.5$ in the definition of the layer-adapted mesh (4). Let $z=\bar{z}+z_\varepsilon$ with each component $\bar{z}$ and z_ε satisfying (3), then one has

$$\|z-\pi^+z\|\leqslant C[N^{-(k+1)}+\sqrt{\varepsilon}\,(N^{-1}\max|\psi'|)^{k+1}] \qquad (11)$$

$$\left(\sum_{j=0}^{N}[\![z-\pi^+z]\!]_j^2\right)^{1/2}\leqslant C(N^{-1}\max|\psi'|)^{k+1/2} \qquad (12)$$

Furthermore, if $\bar{z}\in V_N$, one has

$$\|z-\pi^+z\|\leqslant C\sqrt{\varepsilon}\,(N^{-1}\max|\psi'|)^{k+1} \qquad (13)$$

Proof Denote $\eta_\varsigma=\varsigma-\pi^+\varsigma$ for $\varsigma=\bar{z},\,z_\varepsilon$. From (3) and (10), one has

$$\|\eta_{\bar{z}}\|\leqslant CN^{-(k+1)} \qquad (14)$$

For the monotonic increasing function $\mathrm{e}^{-\alpha(1-x)/\varepsilon},\ x\in[0,1]$, using the stability (8), one has

$$\begin{aligned}\sum_{j=1}^{N/2}\|\eta_{z_\varepsilon}\|_{I_j}^2&\leqslant C\sum_{j=1}^{N/2}\left[\|z_\varepsilon\|_{I_j}^2+h_j|z_\varepsilon(x_{j-1})|^2\right]\\&\leqslant C\sum_{j=1}^{N/2}\left[\|\mathrm{e}^{-\alpha(1-x)/\varepsilon}\|_{I_j}^2+h_j\mathrm{e}^{-2\alpha(1-x_{j-1})/\varepsilon}\right]\\&\leqslant C\int_0^{1-\tau}\mathrm{e}^{-2\alpha(1-x)/\varepsilon}\mathrm{d}x\\&\leqslant C\varepsilon N^{-2\sigma}\end{aligned} \qquad (15)$$

On the refined domain, if $\sigma\geqslant k+1.5$, one obtains from Lemma 1 that

$$\begin{aligned}&\sum_{j=N/2+1}^{N}\|\eta_{z_\varepsilon}\|_{I_j}^2\\&\leqslant C\sum_{j=N/2+1}^{N}\min\{h_j^{2(k+1)}\|z_\varepsilon^{(k+1)}\|_{I_j}^2,\,h_j|z_\varepsilon(x_{j-1})|^2+\|z_\varepsilon\|_{I_j}^2\}\\&\leqslant C\sum_{j=N/2+1}^{N}\min\left\{\left(\frac{h_j}{\varepsilon}\right)^{2(k+1)},1\right\}\|\mathrm{e}^{-\alpha(1-x)/\varepsilon}\|_{I_j}^2\\&\leqslant C\sum_{j=N/2+1}^{N}\varepsilon\left\{\min\{\frac{h_j}{\varepsilon},1\}\mathrm{e}^{-\alpha(1-x_j)/\sigma\varepsilon}\right\}^{2(k+3/2)}\\&\leqslant C\varepsilon\max_{N/2+1\leqslant j\leqslant N}\mathcal{G}_j^{2(k+1)}\sum_{j=N/2+1}^{N}\mathcal{G}_j\\&\leqslant C\varepsilon(N^{-1}\max|\psi'|)^{2(k+1)}\end{aligned} \qquad (16)$$

Consequently, (11) follows from (14) - (16). Note that if $\bar{z} \in V_N$, (13) follows from (15),(16).

By the L^∞ approximation property (10), one has

$$\sum_{j=0}^{N} [\![\eta_{\bar{z}}]\!]_j^2 \leqslant C \sum_{j=1}^{N} \| \eta_{\bar{z}} \|_{L^\infty(I_j)}^2 \leqslant C \sum_{j=1}^{N} N^{-2(k+1)} \leqslant C N^{-(2k+1)}$$

By Lemma 1 and $\sigma \geqslant k+1$ one obtains

$$\begin{aligned}\sum_{j=0}^{N} [\![\eta_{z_\varepsilon}]\!]_j^2 &\leqslant C \sum_{j=N/2+1}^{N} \| \eta_{z_\varepsilon} \|_{L^\infty(I_j)}^2 + C \sum_{j=1}^{N/2} \| \eta_{z_\varepsilon} \|_{L^\infty(I_j)}^2 \\ &\leqslant C \sum_{j=N/2+1}^{N} \min\left\{ h_j^{2(k+1)} \| z_\varepsilon^{(k+1)} \|_{L^\infty(I_j)}^2, \| z_\varepsilon \|_{L^\infty(I_j)}^2 \right\} \\ &\quad + C \sum_{j=1}^{N/2} \| z_\varepsilon \|_{L^\infty(I_j)}^2 \\ &\leqslant C \max_{N/2+1 \leqslant j \leqslant N} \mathcal{G}_j^{2k+1} \sum_{j=N/2+1}^{N} \mathcal{G}_j + C N^{-2\sigma+1} \\ &\leqslant C (N^{-1} \max |\psi'|)^{2k+1}\end{aligned}$$

which leads to (12).

Theorem 1 Let q and $Q \in V_N$ are respectively the solutions of (1) and (5) . Then one has

$$\| q - Q \| \leqslant C \left[N^{-(k+1)} + \sqrt{\varepsilon} \left(N^{-1} \max |\psi'| \right)^{k+1} \right] \quad (17)$$

Furthermore, if $\bar{q} \in V_N$, one has

$$\| q - Q \| \leqslant C \sqrt{\varepsilon} \left(N^{-1} \max |\psi'| \right)^{k+1} \quad (18)$$

Proof For any $r \in V_N$, one has Galerkin orthogonality $B(q-Q;r)=0$ which leads to

$$\begin{aligned}\| \xi \|_{\mathrm{E}}^2 &= B(\xi;\xi) = B(\eta;\xi) \\ &= \varepsilon \sum_{j=0}^{N-1} \eta_j^+ [\![\xi]\!]_j + \langle \eta, \varepsilon \xi' + a\xi \rangle \\ &= \langle \eta, a\xi \rangle \leqslant C \| \eta \| \| a^{1/2} \xi \| \\ &\leqslant C \| \eta \| \| \xi \|_{\mathrm{E}}\end{aligned}$$

Then one gets from (11) that

$$\begin{aligned}\| \xi \| &\leqslant \| \xi \|_{\mathrm{E}} \leqslant C \| \eta \| \\ &\leqslant C \left[N^{-(k+1)} + \sqrt{\varepsilon} \left(N^{-1} \max |\psi'| \right)^{k+1} \right]\end{aligned}$$

Hence,

$$\begin{aligned}\| e \| &\leqslant \| \eta \| + \| \xi \| \leqslant C \| \eta \| \\ &\leqslant C \left[N^{-(k+1)} + \sqrt{\varepsilon} \left(N^{-1} \max |\psi'| \right)^{k+1} \right]\end{aligned}$$

If $\bar{q} \in V_N$, by (13), one has

$$\| e \| \leqslant C \| \eta \| \leqslant C \sqrt{\varepsilon} (N^{-1} \max |\psi'|)^{k+1}$$

Remark 1 Theorem 1 presents a convergence rate $O(N^{-(k+1)} + \sqrt{\varepsilon} \left(N^{-1} \max |\psi'| \right)^{k+1})$ for an equal number of mesh elements in the rough and refined domains. However, it is possible to explore different number of mesh elements in rough and refined domains (denote N_1 and N_2 respectively). Following the similar line, one derives a convergence rate $O(N_1^{-(k+1)} + \sqrt{\varepsilon} \left(N_2^{-1} \max |\psi'| \right)^{k+1})$. Then it is possible to use larger N_2 to balance the influence of $\max|\psi'|$ on the convergence rate and arrive at a convergence $O(N_1^{-(k+1)})$.

3 Numerical Experiments

We perform the DG method (5) on the eight meshes given by Table 1. Set $\sigma = k+1.5$. For the pS-mesh, take $m=2$. For the RS-mesh, take $l=3$. Compute the convergence rate by the formulae

$$r_2 = \frac{\log e^N - \log e^{2N}}{\log 2},$$

$$r_s = \frac{\log e^N - \log e^{2N}}{\log(2\ln N/\ln 2N)}$$

The quantities r_2 and r_s are used to reflect the convergence rates from the error bounds of the forms CN^{-r} and $C(N^{-1}\ln N)^r$, respectively.

Example 1 Consider the problem (1) with $b=1$ and the true solution is set as

$$q(x) = \cos(1-x)\mathrm{e}^{-(1-x)/\varepsilon}$$

As mentioned before, for a large ε, one can use arbitrary mesh with maximum mesh size h and expect a convergence rate $O(h^{k+1})$. In Table 2, we list the numerical results on four meshes. One observes that the convergence rates on uniform mesh and B-mesh are both $O(N^{-(k+1)})$, the convergence rate on S-mesh is $O((N^{-1}\ln N)^{k+1})$, while the convergence rate on BS-mesh is $O(\max\{\varepsilon, N^{-1}\}^{k+1})$ because its maximum mesh size is bounded by $\max\{\varepsilon, N^{-1}\}$.

Table 3 and Table 4 list the L^2-error of the DG method on the eight meshes for $\varepsilon = 10^{-4}$ and $\varepsilon = 10^{-8}$, respectively. One observes for the S-mesh a convergence rate $O((N^{-1}\ln N)^{k+1})$, while for the BS-, mBS-, VS-, B- and mVB- meshes a general convergence rate $O(N^{-(k+1)})$. For the pS-mesh, the convergence rate is a little smaller than k+1 because of the influence of the logarithmic factor (here $\max|\psi'| = (\ln N)^{1/2}$). For the RS-mesh, the convergence rate behaviors as $O(N^{-2(k+1)/3})$ which agrees

Table 2 L^2-error on 4 meshes for Example 1, where $\varepsilon=10^{-2}$

k	N	Uniform-mesh		S-mesh		BS-mesh		B-mesh	
		L^2-error	r_2	L^2-error	r_s	L^2-error	r_2	L^2-error	r_2
1	4	5.81E−02	—	1.76E−02	—	1.64E−02	—	1.66E−02	—
	8	5.08E−02	0.19	6.58E−03	3.41	4.33E−03	1.92	4.31E−03	1.94
	16	3.60E−02	0.50	2.85E−03	2.06	1.16E−03	1.90	1.15E−03	1.91
	32	1.92E−02	0.91	1.16E−03	1.91	3.12E−04	1.89	3.13E−04	1.88
	64	7.37E−03	1.38	4.33E−04	1.93	8.43E−05	1.89	8.62E−05	1.86
	128	2.24E−03	1.72	1.50E−04	1.96	2.54E−05	1.73	2.37E−05	1.86
	256	6.11E−04	1.88	4.97E−05	1.98	1.37E−05	0.89	6.41E−06	1.89
	512	1.59E−04	1.95	1.58E−05	1.99	1.24E−05	0.14	1.68E−06	1.93
	1 024	4.04E−05	1.97	4.91E−06	1.99	1.22E−05	0.02	4.31E−07	1.96
2	4	4.49E−02	—	2.95E−03	—	1.59E−03	—	4.31E−03	—
	8	3.36E−02	0.42	1.45E−03	2.46	3.40E−04	2.22	5.27E−04	3.03
	16	1.66E−02	1.02	5.01E−04	2.63	5.60E−05	2.60	6.75E−05	2.96
	32	5.06E−03	1.71	1.35E−04	2.80	8.09E−06	2.79	8.71E−06	2.95
	64	9.85E−04	2.36	3.06E−05	2.90	1.10E−06	2.89	1.12E−06	2.96
	128	1.47E−04	2.75	6.25E−06	2.95	1.45E−07	2.92	1.43E−07	2.97
	256	1.96E−05	2.90	1.18E−06	2.97	2.50E−08	2.53	1.81E−08	2.98
	512	2.51E−06	2.96	2.12E−07	2.99	1.83E−08	0.45	2.28E−09	2.99
	1 024	3.18E−07	2.98	3.65E−08	2.99	2.03E−08	−0.15	2.87E−10	2.99
3	4	3.19E−02	—	9.93E−04	—	3.90E−04	—	1.56E−03	—
	8	1.92E−02	0.73	3.97E−04	3.19	5.00E−05	2.96	9.10E−05	4.10
	16	6.06E−03	1.66	9.68E−05	3.48	4.40E−06	3.51	5.67E−06	4.01
	32	9.98E−04	2.60	1.68E−05	3.73	3.28E−07	3.75	3.60E−07	3.98
	64	9.74E−05	3.36	2.33E−06	3.87	2.24E−08	3.87	2.28E−08	3.98
	128	7.18E−06	3.76	2.78E−07	3.94	1.54E−09	3.86	1.46E−09	3.97
	256	4.75E−07	3.92	3.01E−08	3.97	6.54E−10	1.24	9.63E−11	3.92
	512	3.04E−08	3.97	3.04E−09	3.99	6.53E−10	0.00	6.41E−12	3.91
	1 024	1.91E−09	3.99	2.91E−10	3.99	6.49E−10	0.01	4.15E−13	3.95

with theoretical prediction (17) in view of l=3 and $\max|\psi'|=N^{1/3}$. Thus, the numerical convergence rate is generally $O((N^{-1}\max|\psi'|)^{k+1})$ for every meshes, which confirms our theoretical convergence rate in Theorem 1.

Furthermore, Figure 1 and Table 5 show that the L^2-error is uniform regarding the singular perturbation parameter in the case that $k=2$ and N=64 except the S-mesh and RS-mesh which are slightly influenced by the factor $\sqrt{\varepsilon}$ as ε is suitably large.

Example 2 We continue example 1 but employ a different true solution

$$q(x)=2-\mathrm{e}^{-(1-x)/\varepsilon}$$

Now the regular component of q is in the finite element space. Let $\varepsilon=10^{-4},10^{-8}$. Tables 6-7 show a general convergence rate $O((N^{-1}\max|\psi'|)^{k+1})$ for each mesh. Furthermore, Figure 2 and Table 8 demonstrate the influence of the factor $\sqrt{\varepsilon}$ on the upper bound of these L^2-errors, which confirms our prediction (18).

Table 3 L^2-error on 8 layer-adapted meshes for Example 1, where $\varepsilon=10^{-4}$

k	N	S-mesh		BS-mesh		mBS-mesh		VS-mesh		pS-mesh		B-mesh		mVB-mesh		RS-mesh	
		L^2-error	r_s	L^2-error	r_2	L^2-error	r_2	L^2-error	r_2	L^2-error	r_2	L^2-error	r_2	L^2-error	r_2	L^2-error	r_2
	4	1.59E−02	—	1.59E−02	—	1.59E−02	—	1.59E−02	—	1.59E−02	—	1.59E−02	—	1.59E−02	—	1.59E−02	—
	8	4.01E−03	4.80	3.98E−03	2.00	3.98E−03	2.00	3.98E−03	2.00	3.98E−03	2.00	3.96E−03	2.00	3.97E−03	2.00	4.00E−03	2.00
	16	1.03E−03	3.36	9.94E−04	2.00	9.94E−04	2.00	9.94E−04	2.00	9.98E−04	2.00	9.91E−04	2.00	9.94E−04	2.00	1.01E−03	1.98
	32	2.73E−04	2.82	2.49E−04	2.00	2.49E−04	2.00	2.49E−04	2.00	2.51E−04	1.99	2.48E−04	2.00	2.49E−04	2.00	2.64E−04	1.94
1	64	7.53E−05	2.52	6.22E−05	2.00	6.22E−05	2.00	6.22E−05	2.00	6.31E−05	1.99	6.20E−05	2.00	6.22E−05	2.00	7.26E−05	1.86
	128	2.15E−05	2.32	1.55E−05	2.00	1.56E−05	2.00	1.56E−05	2.00	1.59E−05	1.99	1.55E−05	2.00	1.56E−05	2.00	2.20E−05	1.73
	256	6.29E−06	2.20	3.90E−06	2.00	3.91E−06	2.00	3.91E−06	2.00	4.01E−06	1.98	3.89E−06	2.00	3.90E−06	2.00	7.39E−06	1.57
	512	1.86E−06	2.12	9.84E−07	1.99	9.87E−07	1.99	9.87E−07	1.99	1.02E−06	1.97	9.82E−07	1.99	9.86E−07	1.99	2.71E−06	1.45
	1 024	5.51E−07	2.07	2.53E−07	1.96	2.54E−07	1.96	2.54E−07	1.96	2.65E−07	1.95	2.53E−07	1.96	2.54E−07	1.96	1.04E−06	1.38
	4	4.97E−04	—	4.30E−04	—	4.34E−04	—	4.34E−04	—	4.53E−04	—	6.32E−04	—	6.35E−04	—	4.68E−04	—
	8	1.54E−04	4.07	6.11E−05	2.81	6.25E−05	2.80	6.25E−05	2.80	7.81E−05	2.54	7.73E−05	3.03	9.72E−05	2.71	1.20E−04	1.96
	16	5.05E−05	2.75	8.48E−06	2.85	8.94E−06	2.80	8.94E−06	2.80	1.41E−05	2.47	9.64E−06	3.00	1.30E−05	2.91	3.30E−05	1.87
	32	1.35E−05	2.81	1.14E−06	2.90	1.25E−06	2.83	1.25E−06	2.83	2.45E−06	2.52	1.21E−06	2.99	1.70E−06	2.93	8.99E−06	1.88
2	64	3.07E−06	2.90	1.48E−07	2.94	1.71E−07	2.87	1.71E−07	2.87	4.04E−07	2.60	1.53E−07	2.99	2.18E−07	2.96	2.38E−06	1.92
	128	6.25E−07	2.95	1.89E−08	2.97	2.29E−08	2.90	2.29E−08	2.90	6.39E−08	2.66	1.92E−08	2.99	2.77E−08	2.98	6.14E−07	1.95
	256	1.18E−07	2.97	2.40E−09	2.98	3.02E−09	2.92	3.02E−09	2.92	9.78E−09	2.71	2.42E−09	2.99	3.49E−09	2.99	1.57E−07	1.97
	512	2.12E−08	2.99	3.04E−10	2.98	3.95E−10	2.94	3.95E−10	2.94	1.46E−09	2.74	3.05E−10	2.99	4.39E−10	2.99	3.96E−08	1.98
	1 024	3.65E−09	2.99	3.87E−11	2.97	5.15E−11	2.94	5.15E−11	2.94	2.14E−10	2.77	3.88E−11	2.97	5.54E−11	2.99	9.95E−09	1.99
	4	1.01E−04	—	4.41E−05	—	4.97E−05	—	4.97E−05	—	6.87E−05	—	1.71E−04	—	1.82E−04	—	8.16E−05	—
	8	3.97E−05	3.26	5.16E−06	3.10	5.83E−06	3.09	5.83E−06	3.09	1.14E−05	2.59	1.02E−05	4.08	1.76E−05	3.38	2.66E−05	1.62
	16	9.68E−06	3.48	4.48E−07	3.53	5.39E−07	3.44	5.39E−07	3.44	1.41E−06	3.01	6.25E−07	4.02	1.19E−06	3.89	5.25E−06	2.34
	32	1.68E−06	3.73	3.32E−08	3.75	4.36E−08	3.63	4.36E−08	3.63	1.45E−07	3.28	3.91E−08	4.00	7.85E−08	3.92	9.20E−07	2.51
3	64	2.33E−07	3.87	2.27E−09	3.87	3.25E−09	3.75	3.25E−09	3.75	1.35E−08	3.43	2.46E−09	3.99	5.06E−09	3.96	1.55E−07	2.57
	128	2.78E−08	3.94	1.49E−10	3.93	2.30E−10	3.82	2.30E−10	3.82	1.16E−09	3.53	1.55E−10	3.99	3.22E−10	3.98	2.53E−08	2.61
	256	3.01E−09	3.97	9.53E−12	3.96	1.58E−11	3.87	1.58E−11	3.87	9.56E−11	3.60	9.71E−12	3.99	2.03E−11	3.99	4.07E−09	2.64
	512	3.04E−10	3.99	6.04E−13	3.98	1.06E−12	3.90	1.06E−12	3.90	7.59E−12	3.65	6.09E−13	3.99	1.27E−12	3.99	6.49E−10	2.65
	1 024	2.91E−11	3.99	3.82E−14	3.98	7.04E−14	3.91	7.04E−14	3.91	5.87E−13	3.69	3.84E−14	3.99	7.98E−14	3.99	1.03E−10	2.66

Table 4 L^2-error on 8 layer-adapted meshes for Example 1, where $\varepsilon = 10^{-8}$

k	N	S-mesh		BS-mesh		mBS-mesh		VS-mesh		pS-mesh		B-mesh		mVB-mesh		RS-mesh	
		L^2-error	r_s	L^2-error	r_2	L^2-error	r_2	L^2-error	r_2	L^2-error	r_2	L^2-error	r_2	L^2-error	r_2	L^2-error	r_2
	4	1.59E−02	—	1.59E−02	—	1.59E−02	—	1.59E−02	—	1.59E−02	—	1.59E−02	—	1.59E−02	—	1.59E−02	—
	8	3.98E−03	4.83	3.98E−03	2.00	3.98E−03	2.00	3.98E−03	2.00	3.98E−03	2.00	3.98E−03	2.00	3.98E−03	2.00	3.98E−03	2.00
	16	9.93E−04	3.42	9.93E−04	2.00	9.93E−04	2.00	9.93E−04	2.00	9.93E−04	2.00	9.93E−04	2.00	9.93E−04	2.00	9.93E−04	2.00
	32	2.48E−04	2.95	2.48E−04	2.00	2.48E−04	2.00	2.48E−04	2.00	2.48E−04	2.00	2.48E−04	2.00	2.48E−04	2.00	2.48E−04	2.00
1	64	6.21E−05	2.71	6.21E−05	2.00	6.21E−05	2.00	6.21E−05	2.00	6.21E−05	2.00	6.21E−05	2.00	6.21E−05	2.00	6.21E−05	2.00
	128	1.55E−05	2.57	1.55E−05	2.00	1.55E−05	2.00	1.55E−05	2.00	1.55E−05	2.00	1.55E−05	2.00	1.55E−05	2.00	1.55E−05	2.00
	256	3.88E−06	2.48	3.88E−06	2.00	3.88E−06	2.00	3.88E−06	2.00	3.88E−06	2.00	3.88E−06	2.00	3.88E−06	2.00	3.88E−06	2.00
	512	9.70E−07	2.41	9.70E−07	2.00	9.70E−07	2.00	9.70E−07	2.00	9.70E−07	2.00	9.70E−07	2.00	9.70E−07	2.00	9.70E−07	2.00
	1 024	2.43E−07	2.36	2.42E−07	2.00	2.42E−07	2.00	2.42E−07	2.00	2.42E−07	2.00	2.42E−07	2.00	2.42E−07	2.00	2.42E−07	2.00
	4	4.03E−04	—	4.03E−04	—	4.03E−04	—	4.03E−04	—	4.03E−04	—	4.03E−04	—	4.03E−04	—	4.03E−04	—
	8	5.12E−05	7.17	5.11E−05	2.98	5.11E−05	2.98	5.11E−05	2.98	5.11E−05	2.98	5.11E−05	2.98	5.11E−05	2.98	5.12E−05	2.98
	16	6.44E−06	5.11	6.42E−06	2.99	6.42E−06	2.99	6.42E−06	2.99	6.42E−06	2.99	6.42E−06	2.99	6.42E−06	2.99	6.42E−06	2.99
	32	8.14E−07	4.40	8.03E−07	3.00	8.03E−07	3.00	8.03E−07	3.00	8.03E−07	3.00	8.03E−07	3.00	8.03E−07	3.00	8.08E−07	2.99
2	64	1.05E−07	4.01	1.00E−07	3.00	1.00E−07	3.00	1.00E−07	3.00	1.00E−07	3.00	1.00E−07	3.00	1.00E−07	3.00	1.03E−07	2.97
	128	1.40E−08	3.73	1.25E−08	3.00	1.25E−08	3.00	1.25E−08	3.00	1.26E−08	3.00	1.25E−08	3.00	1.25E−08	3.00	1.40E−08	2.88
	256	1.96E−09	3.51	1.57E−09	3.00	1.57E−09	3.00	1.57E−09	3.00	1.57E−09	3.00	1.57E−09	3.00	1.57E−09	3.00	2.22E−09	2.66
	512	2.89E−10	3.33	1.96E−10	3.00	1.96E−10	3.00	1.96E−10	3.00	1.97E−10	3.00	1.96E−10	3.00	1.96E−10	3.00	4.41E−10	2.33
	1 024	4.41E−11	3.20	2.45E−11	3.00	2.45E−11	3.00	2.45E−11	3.00	2.46E−11	3.00	2.45E−11	3.00	2.45E−11	3.00	1.02E−10	2.11
	4	2.13E−05	—	2.12E−05	—	2.12E−05	—	2.12E−05	—	2.12E−05	—	2.12E−05	—	2.12E−05	—	2.12E−05	—
	8	1.38E−06	9.50	1.32E−06	4.00	1.32E−06	4.00	1.32E−06	4.00	1.33E−06	4.00	1.32E−06	4.00	1.32E−06	4.00	1.35E−06	3.98
	16	1.27E−07	5.88	8.28E−08	4.00	8.28E−08	4.00	8.28E−08	4.00	8.38E−08	3.99	8.28E−08	4.00	8.28E−08	4.00	9.79E−08	3.78
	32	1.76E−08	4.21	5.17E−09	4.00	5.18E−09	4.00	5.18E−09	4.00	5.36E−09	3.97	5.17E−09	4.00	5.18E−09	4.00	1.06E−08	3.21
3	64	2.35E−09	3.94	3.24E−10	4.00	3.24E−10	4.00	3.24E−10	4.00	3.50E−10	3.94	3.24E−10	4.00	3.24E−10	4.00	1.59E−09	2.73
	128	2.79E−10	3.95	2.02E−11	4.00	2.03E−11	4.00	2.03E−11	4.00	2.33E−11	3.91	2.02E−11	4.00	2.03E−11	4.00	2.54E−10	2.64
	256	3.01E−11	3.98	1.31E−12	3.95	1.32E−12	3.95	1.32E−12	3.95	1.61E−12	3.85	1.31E−12	3.95	1.32E−12	3.95	4.08E−11	2.64
	512	3.18E−12	3.91	3.62E−13	—	3.34E−13	—	3.34E−13	—	3.44E−13	—	3.62E−13	—	3.34E−13	—	6.49E−12	2.65
	1 024	3.63E−13	—	3.57E−13	—	3.37E−13	—	3.37E−13	—	3.38E−13	—	3.57E−13	—	3.37E−13	—	1.08E−12	2.59

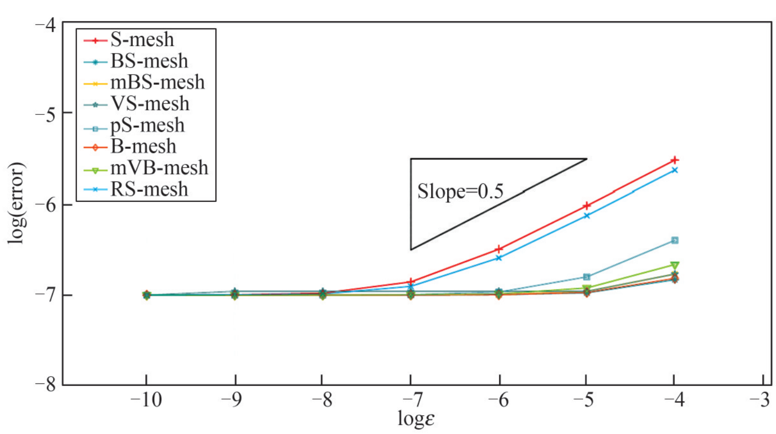

Fig. 1 L^2-error on the singular perturbation parameter for Example 1

Table 5 L^2-error on 8 layer-adapted meshes for Example 1, here k=2 and N=64

ε	S-mesh	BS-mesh	mBS-mesh	VS-mesh	pS-mesh	B-mesh	mVB-mesh	RS-mesh
1.0×10^{-4}	3.07E−06	1.48E−07	1.71E−07	1.71E−07	4.04E−07	1.53E−07	2.18E−07	2.38E−06
1.0×10^{-5}	9.74E−07	1.06E−07	1.10E−07	1.10E−07	1.59E−07	1.07E−07	1.20E−07	7.58E−07
1.0×10^{-6}	3.22E−07	1.01E−07	1.01E−07	1.10E−07	1.08E−07	1.01E−07	1.03E−07	2.58E−07
1.0×10^{-7}	1.40E−07	1.00E−07	1.01E−07	1.10E−07	1.01E−07	1.00E−07	1.01E−07	1.25E−07
1.0×10^{-8}	1.05E−07	1.00E−07	1.00E−07	1.10E−07	1.00E−07	1.00E−07	1.00E−07	1.03E−07
1.0×10^{-9}	1.01E−07	1.00E−07	1.00E−07	1.10E−07	1.00E−07	1.00E−07	1.00E−07	1.01E−07
1.0×10^{-10}	1.00E−07	1.00E−07	1.00E−07	1.00E−07	1.00E−07	1.00E−07	1.00E−07	1.00E−07

Table 6 L^2-error on 8 layer-adapted meshes for Example 2, where $\varepsilon = 10^{-4}$

k	N	S-mesh		BS-mesh		mBS-mesh		VS-mesh		pS-mesh		B-mesh		mVB-mesh		RS-mesh	
		L^2-error	r_s	L^2-error	r_2	L^2-error	r_2	L^2-error	r_2	L^2-error	r_2	L^2-error	r_2	L^2-error	r_2	L^2-error	r_2
	4	8.64E−04	—	5.90E−04	—	6.04E−04	—	6.04E−04	—	6.79E−04	—	1.31E−03	—	1.31E−03	—	7.32E−04	—
	8	5.46E−04	1.59	2.29E−04	1.37	2.35E−04	1.36	2.35E−04	1.36	3.16E−04	1.11	3.28E−04	1.99	4.03E−04	1.70	4.59E−04	0.67
	16	2.70E−04	1.73	7.16E−05	1.68	7.58E−05	1.63	7.58E−05	1.63	1.16E−04	1.45	8.49E−05	1.95	1.12E−04	1.85	2.08E−04	1.14
	32	1.14E−04	1.84	2.02E−05	1.82	2.23E−05	1.76	2.23E−05	1.76	3.83E−05	1.60	2.20E−05	1.95	2.98E−05	1.90	9.06E−05	1.20
1	64	4.28E−05	1.91	5.41E−06	1.90	6.21E−06	1.84	6.21E−06	1.84	1.19E−05	1.69	5.63E−06	1.96	7.74E−06	1.95	3.80E−05	1.25
	128	1.50E−05	1.95	1.40E−06	1.95	1.67E−06	1.89	1.67E−06	1.89	3.53E−06	1.75	1.43E−06	1.98	1.98E−06	1.97	1.56E−05	1.29
	256	4.95E−06	1.97	3.58E−07	1.97	4.41E−07	1.92	4.41E−07	1.92	1.02E−06	1.79	3.61E−07	1.98	4.99E−07	1.98	6.29E−06	1.31
	512	1.58E−06	1.99	9.05E−08	1.98	1.15E−07	1.94	1.15E−07	1.94	2.88E−07	1.82	9.09E−08	1.99	1.25E−07	1.99	2.53E−06	1.32
	1 024	4.90E−07	1.99	2.28E−08	1.99	2.95E−08	1.96	2.95E−08	1.96	8.02E−08	1.84	2.28E−08	1.99	3.15E−08	2.00	1.01E−06	1.32
	4	2.91E−04	—	1.51E−04	—	1.63E−04	—	1.63E−04	—	2.09E−04	—	4.90E−04	—	4.93E−04	—	2.39E−04	—
	8	1.45E−04	2.41	3.36E−05	2.17	3.61E−05	2.18	3.61E−05	2.18	5.91E−05	1.82	5.83E−05	3.07	8.30E−05	2.57	1.09E−04	1.13
	16	5.01E−05	2.63	5.57E−06	2.59	6.25E−06	2.53	6.25E−06	2.53	1.25E−05	2.24	7.25E−06	3.01	1.13E−05	2.87	3.23E−05	1.75
	32	1.35E−05	2.80	8.06E−07	2.79	9.65E−07	2.69	9.65E−07	2.69	2.31E−06	2.44	9.16E−07	2.98	1.50E−06	2.91	8.95E−06	1.85
2	64	3.06E−06	2.90	1.09E−07	2.89	1.39E−07	2.79	1.39E−07	2.79	3.92E−07	2.56	1.16E−07	2.98	1.94E−07	2.95	2.38E−06	1.91
	128	6.25E−07	2.95	1.42E−08	2.94	1.92E−08	2.86	1.92E−08	2.86	6.27E−08	2.64	1.46E−08	2.99	2.47E−08	2.97	6.14E−07	1.95
	256	1.18E−07	2.97	1.82E−09	2.97	2.58E−09	2.89	2.58E−09	2.89	9.65E−09	2.70	1.84E−09	2.99	3.12E−09	2.99	1.56E−07	1.97
	512	2.12E−08	2.99	2.30E−10	2.98	3.41E−10	2.92	3.41E−10	2.92	1.45E−09	2.74	2.32E−10	2.99	3.91E−10	2.99	3.96E−08	1.98
	1 024	3.65E−09	2.99	2.89E−11	2.99	4.46E−11	2.94	4.46E−11	2.94	2.12E−10	2.77	2.90E−11	3.00	4.90E−11	3.00	9.95E−09	1.99
	4	9.92E−05	—	3.87E−05	—	4.50E−05	—	4.50E−05	—	6.54E−05	—	1.70E−04	—	1.81E−04	—	7.88E−05	—
	8	3.97E−05	3.18	4.99E−06	2.96	5.68E−06	2.99	5.68E−06	2.99	1.13E−05	2.53	1.01E−05	4.08	1.75E−05	3.37	2.66E−05	1.57
	16	9.68E−06	3.48	4.40E−07	3.50	5.33E−07	3.41	5.33E−07	3.41	1.41E−06	3.01	6.19E−07	4.02	1.19E−06	3.88	5.25E−06	2.34
	32	1.68E−06	3.73	3.28E−08	3.75	4.33E−08	3.62	4.33E−08	3.62	1.45E−07	3.28	3.87E−08	4.00	7.84E−08	3.92	9.20E−07	2.51
3	64	2.33E−07	3.87	2.24E−09	3.87	3.23E−09	3.74	3.23E−09	3.74	1.35E−08	3.43	2.44E−09	3.99	5.05E−09	3.95	1.55E−07	2.57
	128	2.78E−08	3.94	1.47E−10	3.93	2.29E−10	3.82	2.29E−10	3.82	1.16E−09	3.53	1.53E−10	3.99	3.21E−10	3.98	2.53E−08	2.61
	256	3.01E−09	3.97	9.44E−12	3.96	1.58E−11	3.86	1.58E−11	3.86	9.56E−11	3.60	9.63E−12	3.99	2.02E−11	3.99	4.07E−09	2.64
	512	3.04E−10	3.99	5.98E−13	3.98	1.06E−12	3.90	1.06E−12	3.90	7.59E−12	3.65	6.04E−13	4.00	1.27E−12	3.99	6.49E−10	2.65
	1 024	2.91E−11	3.99	3.78E−14	3.98	7.02E−14	3.91	7.02E−14	3.91	5.87E−13	3.69	3.81E−14	3.99	7.96E−14	4.00	1.03E−10	2.66

Table 7 L^2-error on 8 layer-adapted meshes for Example 2, where $\varepsilon = 10^{-8}$

k	N	S-mesh		BS-mesh		mBS-mesh		VS-mesh		pS-mesh		B-mesh		mVB-mesh		RS-mesh	
		L^2-error	r_s	L^2-error	r_2	L^2-error	r_2	L^2-error	r_2	L^2-error	r_2	L^2-error	r_2	L^2-error	r_2	L^2-error	r_2
	4	8.64E−06	—	5.90E−06	—	6.04E−06	—	6.04E−06	—	6.79E−06	—	1.19E−05	—	1.34E−05	—	7.32E−06	—
	8	5.46E−06	1.59	2.29E−06	1.37	2.35E−06	1.36	2.35E−06	1.36	3.16E−06	1.11	3.17E−06	1.91	4.42E−06	1.60	4.59E−06	0.67
	16	2.70E−06	1.73	7.16E−07	1.68	7.58E−07	1.63	7.58E−07	1.63	1.16E−06	1.45	8.39E−07	1.92	1.23E−06	1.85	2.08E−06	1.14
	32	1.14E−06	1.84	2.02E−07	1.82	2.23E−07	1.76	2.23E−07	1.76	3.83E−07	1.60	2.19E−07	1.94	3.29E−07	1.90	9.06E−07	1.20
1	64	4.28E−07	1.91	5.41E−08	1.90	6.21E−08	1.84	6.21E−08	1.84	1.19E−07	1.69	5.62E−08	1.96	8.54E−08	1.94	3.80E−07	1.25
	128	1.50E−07	1.95	1.40E−08	1.95	1.67E−08	1.89	1.67E−08	1.89	3.53E−08	1.75	1.43E−08	1.97	2.18E−08	1.97	1.56E−07	1.29
	256	4.95E−08	1.97	3.58E−09	1.97	4.41E−09	1.92	4.41E−09	1.92	1.02E−08	1.79	3.62E−09	1.98	5.52E−09	1.98	6.29E−08	1.31
	512	1.58E−08	1.99	9.05E−10	1.98	1.15E−09	1.94	1.15E−09	1.94	2.88E−09	1.82	9.10E−10	1.99	1.39E−09	1.99	2.53E−08	1.32
	1 024	4.90E−09	1.99	2.28E−10	1.99	2.95E−10	1.96	2.95E−10	1.96	8.02E−10	1.84	2.28E−10	1.99	3.48E−10	2.00	1.01E−08	1.32
	4	2.91E−06	—	1.51E−06	—	1.63E−06	—	1.63E−06	—	2.09E−06	—	3.98E−06	—	5.33E−06	—	2.39E−06	—
	8	1.45E−06	2.41	3.36E−07	2.17	3.61E−07	2.18	3.61E−07	2.18	5.91E−07	1.82	5.28E−07	2.91	9.52E−07	2.49	1.09E−06	1.13
	16	5.01E−07	2.63	5.57E−08	2.59	6.25E−08	2.53	6.25E−08	2.53	1.25E−07	2.24	6.95E−08	2.93	1.31E−07	2.86	3.23E−07	1.75
	32	1.35E−07	2.80	8.06E−09	2.79	9.65E−09	2.69	9.65E−09	2.69	2.31E−08	2.44	9.00E−09	2.95	1.74E−08	2.91	8.95E−08	1.85
2	64	3.06E−08	2.90	1.09E−09	2.89	1.39E−09	2.79	1.39E−09	2.79	3.92E−09	2.56	1.15E−09	2.97	2.25E−09	2.95	2.38E−08	1.91
	128	6.25E−09	2.95	1.42E−10	2.94	1.92E−10	2.86	1.92E−10	2.86	6.27E−10	2.64	1.46E−10	2.98	2.87E−10	2.97	6.14E−09	1.95
	256	1.18E−09	2.97	1.82E−11	2.97	2.58E−11	2.89	2.58E−11	2.89	9.65E−11	2.70	1.84E−11	2.99	3.62E−11	2.99	1.57E−09	1.97
	512	2.12E−10	2.99	2.32E−12	2.97	3.42E−12	2.92	3.42E−12	2.92	1.45E−11	2.74	2.35E−12	2.97	4.56E−12	2.99	3.96E−10	1.98
	1 024	3.67E−11	2.99	4.55E−13	—	5.53E−13	—	5.53E−13	—	2.15E−12	2.75	4.65E−13	—	6.58E−13	—	9.95E−11	1.99
	4	9.92E−07	—	3.87E−07	—	4.50E−07	—	4.50E−07	—	6.54E−07	—	1.40E−06	—	2.15E−06	—	7.88E−07	—
	8	3.97E−07	3.18	4.99E−08	2.95	5.68E−08	2.99	5.68E−08	2.99	1.13E−07	2.53	9.03E−08	3.95	2.09E−07	3.36	2.66E−07	1.57
	16	9.68E−08	3.48	4.40E−09	3.50	5.33E−09	3.41	5.33E−09	3.41	1.41E−08	3.01	5.86E−09	3.95	1.44E−08	3.86	5.25E−08	2.34
	32	1.68E−08	3.73	3.28E−10	3.75	4.33E−10	3.62	4.33E−10	3.62	1.45E−09	3.28	3.77E−10	3.96	9.55E−10	3.92	9.20E−09	2.51
3	64	2.33E−09	3.87	2.24E−11	3.87	3.23E−11	3.74	3.23E−11	3.74	1.35E−10	3.43	2.41E−11	3.97	6.17E−11	3.95	1.55E−09	2.57
	128	2.78E−10	3.94	1.51E−12	3.89	2.31E−12	3.81	2.31E−12	3.81	1.16E−11	3.53	1.55E−12	3.95	3.93E−12	3.97	2.53E−10	2.61
	256	3.01E−11	3.97	3.68E−13	—	3.82E−13	—	3.82E−13	—	1.00E−12	3.53	3.54E−13	—	4.05E−13	—	4.07E−11	2.64
	512	3.18E−12	3.91	3.53E−13	—	3.24E−13	—	3.24E−13	—	3.35E−13	—	3.73E−13	—	3.48E−13	—	6.49E−12	2.65
	1 024	3.63E−13	—	3.57E−13	—	3.37E−13	—	3.37E−13	—	3.38E−13	—	3.56E−13	—	3.38E−13	—	1.08E−12	2.59

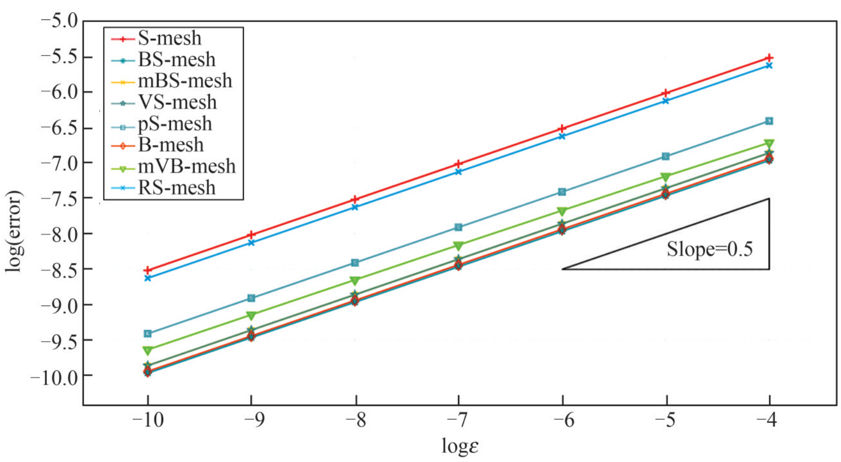

Fig. 2 L^2-error on the singular perturbation parameter for Example 2

Table 8 L^2-error on 8 layer-adapted meshes for Example 2, here k=2 and N=64

ε	S-mesh	BS-mesh	mBS-mesh	VS-mesh	pS-mesh	B-mesh	mVB-mesh	RS-mesh
1.0×10^{-4}	3.06E−06	1.09E−07	1.39E−07	1.39E−07	3.92E−07	1.16E−07	1.94E−07	2.38E−06
1.0×10^{-5}	9.69E−07	3.45E−08	4.40E−08	4.40E−08	1.24E−07	3.67E−08	6.51E−08	7.52E−07
1.0×10^{-6}	3.06E−07	1.09E−08	1.39E−08	1.39E−08	3.92E−08	1.16E−08	2.14E−08	2.38E−07
1.0×10^{-7}	9.69E−08	3.45E−09	4.40E−09	4.40E−09	1.24E−08	3.66E−09	6.97E−09	7.52E−08
1.0×10^{-8}	3.06E−08	1.09E−09	1.39E−09	1.39E−09	3.92E−09	1.15E−09	2.25E−09	2.38E−08
1.0×10^{-9}	9.69E−09	3.45E−10	4.40E−10	4.40E−10	1.24E−09	3.63E−10	7.25E−10	7.52E−09
1.0×10^{-10}	3.06E−09	1.09E−10	1.39E−10	1.39E−10	3.92E−10	1.15E−10	2.33E−10	2.38E−09

References

[1] Roos H G, Stynes M, Tobiska L. *Numerical Methods for Singularly Perturbed Differential Equations*[M]. Berlin: Springer-Verlag, 1996.

[2] Stynes M, Stynes D. *Convection-diffusion Problems*: *An Introduction to Their Analysis and Numerical Solution*[M]. Halifax: American Mathematical Society, 2018.

[3] Miller J J H, Riordan E O, Shishkin G I. *Fitted Numerical Methods for Singular Perturbation Problems*: *Error Estimates in the Maximum Norm for Linear Problems in One and Two Dimensions*[M]. Singapore: World Scientific, 1996.

[4] Reed W H, Hill T R. *Triangular Mesh Methods for the Neutron Transport Equation*[M]. Los Alamos: Los Alamos Scientific Laboratory, 1973.

[5] Cockburn B. Discontinuous Galerkin methods for convection-dominated problems, in high-order methods for computational physics[C]//*Lecture Notes in Computational Science and Engineering.* Berlin: Springer-Verlag, 1999, **9**: 69-224.

[6] Xie Z Q, Zhang Z Z, Zhang Z M. A numerical study of uniform superconvergence of LDG method for solving singularly perturbed problems[J]. *J Comput Math*, 2009, **27**(2-3): 280-298.

[7] Zhu H, Zhang Z. Convergence analysis of the LDG method applied to singularly perturbed problems[J]. *Numerical Methods Partial Differential Equation*, 2013, **29**(2): 396-421.

[8] Zhu H, Zhang Z. Uniform convergence of the LDG method for a singularly perturbed problem with the exponential boundary layer[J]. *Math Comp*, 2014, **286**(83): 635-663.

[9] Cheng Y, Song C J, Mei Y J. Local discontinuous Galerkin method for time-dependent singularly perturbed semilinear reaction-diffusion problems[J]. *Comput Methods Appl Math*, 2021, **21**(1): 31-52.

[10] Cheng Y, Zhang Q, Wang H J. Local analysis of the local discontinuous Galerkin method with the generalized alternating numerical flux for two-dimensional singularly perturbed problem[J]. *Int Numer Anal Mod*, 2018, **15**(6): 785-810.

[11] Cheng Y. On the local discontinuous Galerkin method for singularly perturbed problem with two parameters[J]. *J Comput Appl Math*, 2021, **392**: 113485.

[12] Cheng Y, Mei Y J, Roos H G. The local discontinuous Galerkin method on layer-adapted meshes for time-dependent singularly perturbed convection-diffusion problems[J]. *Comput Math Appl*, 2022, **117**: 245-256.

[13] Linß T. Layer-adapted meshes for convection-diffusion problems[J]. *Comput Methods Appl Mech Engrg*, 2003, **192**: 9-10.

[14] Roos H G. Layer-adapted grids for singular perturbation problems[J]. *Z Angew Math Mech*, 1998, **78**: 291-309.

[15] Xie Z Q, Zhang Z M. Uniform superconvergence analysis of the discontinuous Galerkin method for a singularly perturbed problems in 1-D[J]. *Math Comp*, 2010, **79**(269): 35-45.

[16] Ciarlet P. *The Finite Element Method for Elliptic Problem*[M]. Amsterdam: North-Holland, 1975.

□